Acta of Bioengineering and Biomechanics
Vol. 13, No. 2, 2011

Original paper

Comparative analysis of ventricular assist devices (POLVAD and POLVAD_EXT) based on multiscale FEM model

ANDRZEJ MILENIN, MAGDALENA KOPERNIK*

Department of Applied Computer Science and Modelling, AGH University of Science and Technology, Kraków.

The prosthesis – pulsatory ventricular assist device (VAD) – is made of polyurethane (PU) and biocompatible TiN deposited by pulsed laser deposition (PLD) method. The paper discusses the numerical modelling and computer-aided design of such an artificial organ. Two types of VADs: POLVAD and POLVAD_EXT are investigated. The main tasks and assumptions of the computer program developed are presented. The multiscale model of VAD based on finite element method (FEM) is introduced and the analysis of the stress–strain state in macroscale for the blood chamber in both versions of VAD is shown, as well as the verification of the results calculated by applying ABAQUS, a commercial FEM code. The FEM code developed is based on a new approach to the simulation of multilayer materials obtained by using PLD method. The model in microscale includes two components, i.e., model of initial stresses (residual stress) caused by the deposition process and simulation of active loadings observed in the blood chamber of POLVAD and POLVAD_EXT. The computed distributions of stresses and strains in macro- and microscales are helpful in defining precisely the regions of blood chamber, which can be defined as the failure-source areas.

Key words: *finite element method* (*FEM*), *ventricular assist device* (*VAD*), *residual stress, inverse analysis, representative volume element* (*RVE*), *titanium nitride* (*TiN*)

1. Introduction

Ventricular assist device (VAD) is an artificial organ used to treat heart diseases. Efforts are made to develop such a device that is biocompatible, durable, low-energy consuming, allows monitoring and does not introduce changes into the blood morphology [1]. The walls of the ventricular assist device are covered with a TiN nanocoating using pulsed laser deposition to improve the biocompatibility and the surface properties of the device [2].

The implementation of VAD proves quite difficult because of the following problems:

i) The damage to nanocoating is possible, hence the stress–strain state must be analyzed in microscale. The analysis proposed can be based on efficient methodology – a multiscale conception of FEM. The solutions of this task are: multiscale approach and FEM code proposed in [3]. Consequently, the developed FEM macromodel of VAD is a solid part of FSI (fluid structure interaction) solution [4], [5].

ii) The mechanical properties of TiN nanocoating have to be determined, therefore, the idea of inverse analysis is used. In fact, the mechanical properties of nanocoating are measured in experimental nanotests and using imaging techniques of nanostructures. However, these tests give average values of properties and this information is not sufficient for advanced design of ventricular assist devices. To eliminate this constraint the multiscale modelling is applied [6]. The solution developed is focused on the application and combination of methods such as finite element method, multiscale approach and inverse analysis.

* Corresponding author: Magdalena Kopernik, Department of Applied Computer Science and Modelling, Faculty of Metals Engineering and Industrial Computer Science, AGH University of Science and Technology, al. Mickiewicza 30, 30-059 Kraków, Poland. Tel. +48 (12) 617 26 15, fax +48 (12) 617 29 21, e-mail: kopernik@agh.edu.pl

Received: February 8th, 2011
Accepted for publication: April 5th, 2011

These methods are helpful in predicting failure zones in the material of the ventricular assist device and then, they allow the local behaviour of nanocoating to be analyzed in microscale. Furthermore, it is possible to identify the parameters of the rheological model of nanocoating and to account for the residual stresses [7] which result from the growth process of nanomaterial [8].

The goal of the present paper is to develop a numerical model of the pulsatory ventricular assist device with the option of a local multiscale modelling and comparative analysis of ventricular assist devices (POLVAD and POLVAD_EXT) based on the multiscale FEM model.

In macroscale, the FEM solid problem is focused on strain and stress analysis for two versions of macromodel of VAD's blood chamber (POLVAD and POLVAD_EXT) with the option of local strain and stress analysis in microscale (in representative volume element RVE). In the micromodel, residual stress distribution is taken into account. Additionally, the results obtained in macroscale for both versions of VAD are verified by applying the commercial FEM code of ABAQUS.

2. Material and methods

2.1. Materials

Titanium nitride coating is deposited on the whole outer surface of the VAD's blood chamber made of polyurethane. In linear elastic zone, the parameters of nonlinear elastic polyurethane, which are further used in simulations, are Young's modulus E = 423 MPa and Poisson's ratio ν = 0.4.

The polymer itself exhibits the change in stiffness in a long-term clinical application, therefore, its surface should be modified. Thus, titanium nitride and/or titanium carbonitride coatings are deposited also by the PLD method. The biocompatible properties of these coatings were proved in [2], [9]. Additionally, recent studies extended the view to promising biocompatible parameters of TiN and TiCN coatings deposited by other than PLD physical deposition methods. Many works dedicated to biocompatibility of these coatings confirm the results obtained in [2], [9], but also more biocompatible parameters were measured in [1], [10]–[12]. Identification of the mechanical properties of TiN is based on experimental tests (nanoindention test) and inverse analysis [13].

2.2. Experimental methods

An understanding of the mechanical properties of nanomaterials, which are used in the VADs, is crucial for the accuracy of numerical simulations. In the last two decades, there has been developed a considerable interest in the mechanical characterization of coatings using nanoindentation test [14]. Standard experimental methods used in macroscale are not recommended by specialists to nanocoatings. Nanoindentation tests [14] are performed in load-controlled mode using appropriate experimental system and indenters. The nanoindentation test gives the information about key mechanical parameters such as: hardness, reduced elastic modulus, creep resistance and temperature-dependent properties. No other known nanotechnique provides information about both elastic and plastic properties of coatings. However, these properties do not describe the complete material models of coatings. Due to strong inhomogeneities of the tests, extracting these additional model parameters from the tests is difficult. Therefore, additional attempts to develop the numerical model of nanoindentation test are still undertaken.

The example of the results obtained in nanoindentation test and the model are presented in figure 1 [13]. The force–displacement data is measured in nanoindentation test for TiN nanocoating deposited by PLD. The characteristic of data representing nanoindentation test allows expecting the elastic-plastic properties of TiN coating and, therefore, the bilinear elastic-plastic material model presented in upper part of figure 1 is selected for TiN. The parameters of the material model of TiN (figure 1) were identified in inverse analysis by using a 2D model of nanoindentation test. They are as follows: ε_1 = 0.009, σ_1 = 2.614 GPa, ε_2 = 0.166 and

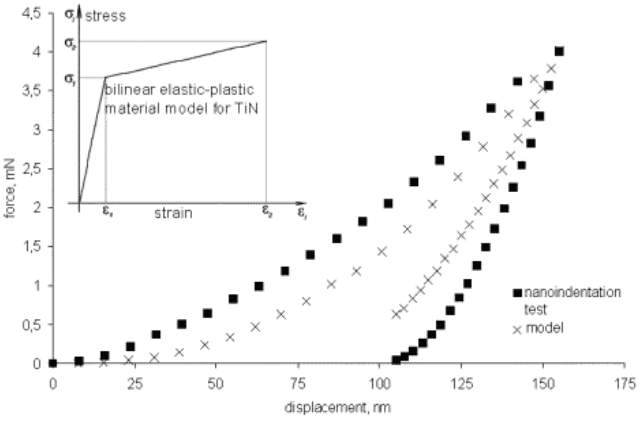

Fig. 1. Force–displacement data of nanoindentation test and model, on the left upper side – material model selected for TiN [13]

σ_2 = 9.107 GPa. According to this analysis, the calculated elastic modulus of TiN is 290 GPa. The elastic modulus obtained is within the range of the values given in literature review shown in [13].

According to [7] residual stresses in coatings produced by PVD (physical vapour deposition) technique result from the contribution of thermal, intrinsic and extrinsic stresses. Tensile intrinsic stresses are usually observed in not fully dense films deposited by thermal evaporation from non-energetic particles. Compressive intrinsic stresses develop in relatively dense films deposited at low temperatures under energetic particle bombardment.

The comparison between the results given in the literature and those obtained for biocompatible TiN nanocoating deposited on PU by using PLD method shown in [13] leads to the conclusion that compressive residual stresses are higher when TiN nanocoating is deposited by the PLD method. The differences in residual stresses for various thicknesses of TiN nanocoating can be as large as 2.4 GPa. High compressive residual stresses observed in many studies of these materials are attributed to the influence of surface tension and may be due to the influence of the conditions on the layer formation. Therefore, the compressive residual stress distribution was introduced as the initial stress into the model of nanoindentation test [13].

The review of major models proposed in the literature to explain the generation of residual stresses in PVD films was prepared by PAULEAU [7]. For example, the method selected in [13] to calculate the residual stress in biocomaptible TiN nanocoating deposited on VADs leads to substituting the Stoney's equation on the basis of the observations of TEM (Transmission Electron Microscopy) images.

2.3. Multiscale FEM solution

In the present paper, the multiscale model of VAD composed of macro- and micromodels is designed in two stages (shown in figure 2): residual stress modelling and active loading modelling. Both stages are based on the FEM code developed by MILENIN and KOPERNIK [3]. In the first stage (figure 2a), the residual stress is reached by applying experimental results and the inverse method in microscale. In the second step (figure 2b), the computed stress and strain states are used as initial values for the analysis of the influence of working loadings on the material of VAD's blood chamber. In this stage, boundary conditions from the solution in microscale are applied to macroscale.

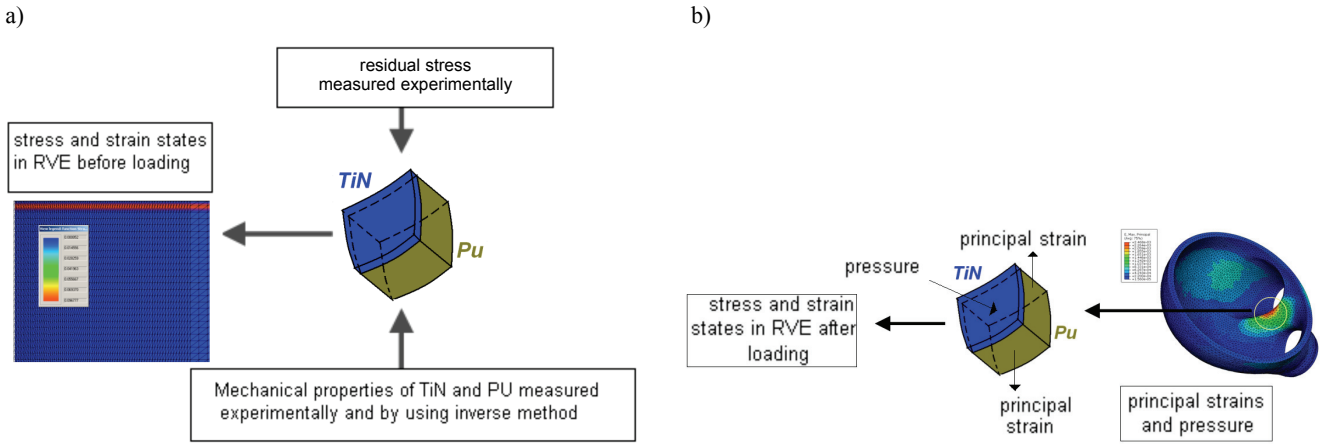

Fig. 2. General conception of multiscale model of VAD blood chamber: residual stress modelling (a) and active loading modelling (b)

The multiscale approach suggested is classified as an upscaling method [15] based on FEM solutions in two different scales for the analysis of phenomena occurring in the nanocoatings due to loading the ventricular assist device in the macroscale. Similar solution, based on the FEM method combined with the representative volume element approach, was proposed in [16] to simulate the influence of colony composed of ferrite and cementite on the macroscopic behaviour during wire drawing.

2.3.1. Bases of macroscale solution

The basic conception of FEM for elastic and elastic-plastic problems is widely described, for example, in [17]. FEM has been implemented in many works dedicated to modelling the following processes observed in VADs and human heart:

i) Blood flow in different phases of VAD work [18].

ii) The modelling of human heart valve function [19].

iii) The multiscale modelling of fibre structure of human heart [19].

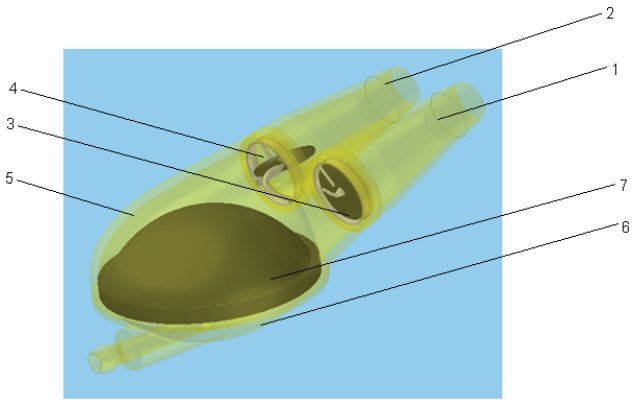

Fig. 3. POLVAD: 1 – inlet connector, 2 – outlet connector, 3 – inlet valve, 4 – outlet valve, 5 – pneumatic chamber, 6 – blood chamber

The types of VAD investigated in the present paper are unique because of deposited nanocoating, which is not done by other researchers. Consequently, there is a lack of data for a solid model of VAD composed of substrate and nanocoating. The developed model of Polish POLVAD is described in [20]. The first construction of VAD (POLVAD) during ejection phase and its main parts are shown in figure 3. POLVAD is a pneumatically driven, membrane type (U-shaped) blood pump developed in the Institute of Heart Prostheses in Zabrze, Poland, to support patients with heart failure during recovery or as a bridge to transplantation. Mechanical valves (commercial Medtronic, Moll's or polyurethane valve) are placed in inlet and outlet connectors. The second type of VAD (POLVAD_EXT) has similar parts of construction, but the difference lies in the design of connectors and their orientation relative to blood chamber (figure 4). The used geometries of VADs are created and refined in CAD program (figure 4) by using the methodology developed. The geometries applied in the FEM models of both VADs are simplified. The final model of the geometry of chamber is composed of two main parts: the top pneumatic chamber and the bottom blood chamber, as well as two channels: reduced connectors.

The tasks of macromodel are as follows:

i) Determination of the areas of blood chamber with the greatest tendency to failure; these areas are further taken into account in microscale model.

ii) The strain–stress state reached during loading in macromodel is introduced into micromodel as boundary conditions.

The main assumptions of finite element solution in macroscale can be itemized as follows:

i) The nonlinearity in elastic deformation process of blood chamber is a result of nonlinear mechanical properties of polyurethane and deposition of the nanocoatings which generates additional initial stress (residual stress).

ii) In macroscale, the VAD deformation is considered as a 3D problem. Thus, the defined boundary problem of the theory of nonlinear elasticity is composed of the groups of equations described in [21].

The bases of solution are:

i) In the case of small nonlinearity of material, the effective Young's modulus is assumed to have a constant value. In the plastic zone of deformation, the modulus of plasticity replaces the Young's modulus. The modulus of plasticity is given by:

$$E' = \frac{\sigma_i}{\varepsilon_i}. \tag{1}$$

ii) The components of stiffness matrix $[K]$ and complete load vector $\{F\}$ are expressed by the following equations:

$$[K_e] = \int_{V_e} [B]^T [D][B] dV, \tag{2}$$

$$\{F_e\} = -\int_{S_e} [\overline{N}]^T \{p\} dS, \tag{3}$$

a) b)

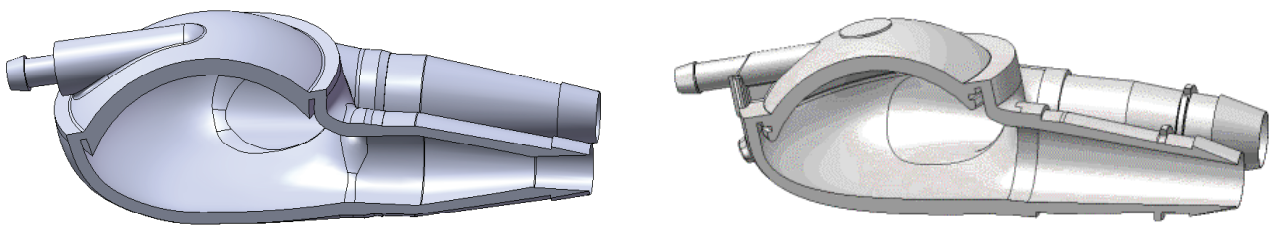

Fig. 4. Cross-sections of CAD models for: POLVAD (a) and POLVAD_EXT(b)

where: S – contact surface, $\{p\}$ – pressure inside VAD, $[B]$ – matrix containing the derivatives of shape functions, $[D]$ – matrix containing the appropriate material properties (E, ν), $[\overline{N}]$ – matrix of shape functions of finite element, V – volume, V_e – volume of current finite element e, S_e – contact surface between current element and blood.

iii) The boundary conditions in macromodel are as follows: distribution of blood pressure p = 16 kPa (maximum physiological blood pressure in the ventricle) on the inner surface of blood chamber, fixed inlets of both connectors of blood chamber (no displacement, no loading) and not fixed surfaces in outer upper part of blood chamber (not fixed surfaces, no loading).

About 30 000 elements were used to solve the boundary problem for the macromodels of POLVAD and POLVAD_EXT (figure 4) and the FEM mesh (figure 5) was generated by algorithms [3], [22] which allowed the boundary conditions (automatic fragmentation of FEM mesh) to be set. The tetrahedron element and the five-point scheme of integration were used.

which belongs this nanostructure. The latter assumption means that the averages of all the gradients vanish in the RVE. The method is based on the principle of volume averaging, leading to the definition of the macrostress tensor in the form:

$$\overline{\sigma} = \frac{1}{V_{\mathrm{RVE}}} \int_{V_{\mathrm{RVE}}} \sigma dV, \tag{4}$$

where $\overline{\sigma}$ is n average stress; the integration is carried out over the RVE with the volume V_{RVE}.

For example, the theory of small elastic-plastic deformations is considered in the modelling of TiN nanocoating. The well-posed problem in the microscale also requires the equality of macrowork with the average volume of microwork:

$$\overline{\sigma} \cdot \overline{\varepsilon} = \frac{1}{V_{\mathrm{RVE}}} \int_{V_{\mathrm{RVE}}} \sigma \varepsilon dV, \tag{5}$$

which is known as the Hill–Mandel macrohomogeneity condition [25] and where $\overline{\varepsilon}$ is an average strain.

a)

b)

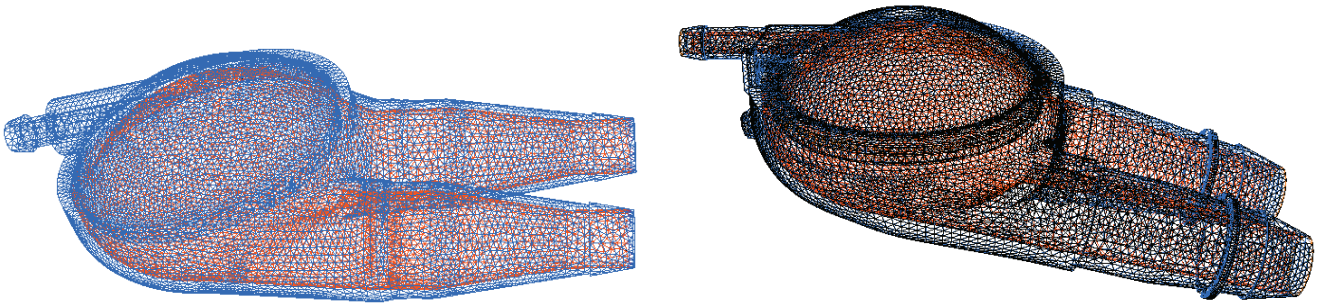

Fig. 5. 3D FEM models of blood chambers of POLVAD [3] (a) and POLVAD_EXT (b)

2.3.2. Bases of microscale solution

Multiscale FEM belongs to the group of homogenization methods, so that it is applicable only in the case of statistically uniform materials [23], [24]. For this kind of materials, it is typical that they possess a representative volume element (RVE), whose analysis yields the effective material parameters, but the limiting condition is that the ratio of the characteristic length of RVE to that of the simulated body has to tend to zero. The representative volume element is an intermediate scale between the nano- and the macroscopic ones. Inhomogeneities of the nanostructure are supposed to be small compared to that of the RVE, and the RVE should be small compared to the item, to

Equation (4) is satisfied by three types of boundary conditions in the microscale: static, kinematic and periodic. In periodic boundary conditions, the displacement components perpendicular to the side of the RVE are imposed, but those parallel to the side are let free. In this case, each side of RVE is a symmetric plane. According to [26], it appears that the best are periodic boundary conditions using an average computed on the whole mesh.

Considering the introduced RVE approach, the following microscale model of the wall of VAD is proposed. The representative volume element is composed of substrate (polyurethane) material layer and deposited TiN nanocoating. In the micromodel, the shape of surface was modelled by sinusoidal function

with the parameters obtained from microscopic examination of real nanocoatings [13]. The thickness of TiN nanocoating is 350 nm.

The bases of solution:

i) The relation between stresses and strains [17] is written using the matrix (vector) definition:

$$\{\sigma\} = [D]\{\varepsilon\} - [D]\{\varepsilon_{0\,\mathrm{res}}\}, \tag{6}$$

where: $\{\varepsilon_{0\,\mathrm{res}}\}$ – residual strains; $\{\sigma\}$ and $\{\varepsilon\}$ – stress and strain tensors, respectively.

ii) The variational principle of the nonlinear elastic and elastic-plastic theory leads to the following functional form of finite element e:

$$W_e = \int_{V_e} \frac{1}{2}\{U\}^T[B]^T[D][B]\{U\}dV - \int_{V_e} \{U\}^T[B]^T[D]\{\varepsilon_{0\,\mathrm{res}}\}dV - \int_{S_e} \{U\}^T[\overline{N}]^T\{p\}dS, \tag{7}$$

where: $\{U\}$ – displacement vector in nodes of elements. In order to linearize this functional for nonlinear problem, the effective Young's modulus E' (equation (1)) is used instead of the Young's modulus in the elastic zone.

iii) The stiffness matrix $[K]$ is the same as in equation (2) and load vector $\{F\}$ is written in the form:

$$\{F\} = -\int_V [B]^T[D]\{\varepsilon_{0\,\mathrm{res}}\}dV - \int_S [\overline{N}]^T\{p\}dS. \tag{8}$$

iv) The collocated distribution of $\varepsilon_{0\,\mathrm{res}}$ is indentified on the basis of the minimization of the following function:

$$R = \sum_{e=1}^{N_e} \int_{V_e} [\sigma_{0\,\mathrm{res}}(\varepsilon_{0\,\mathrm{res}}) - \overline{\sigma}_{0\,\mathrm{res}}]^2, \tag{9}$$

where: e – number of current finite element, N_e – number of finite elements in zone with residual stress, $\overline{\sigma}_{0\,\mathrm{res}}$ – experimental value of residual stress in current finite element e ($\overline{\sigma}_{0\,\mathrm{res}}$ = 0.5 GPa is assumed for TiN nanocoating), $\sigma_{0\,\mathrm{res}}(\varepsilon_{0\,\mathrm{res}})$ – calculated distribution of residual stresses as function of $\varepsilon_{0\,\mathrm{res}}$.

The experimental residual stress is interpreted as an average stress and localized in a TiN nanocoating. After determining $\varepsilon_{0\,\mathrm{res}}$ distribution, the simulations of loading and unloading stages of blood chamber of VAD in microscale are possible.

The boundary conditions for the RVE are modelled according to the following principles. The deformation tensor is obtained from the macromodel. Therefore, a 3D boundary problem of the RVE deformation is applied in a 2D plane strain problem with the nonzero value of ε_2. The value of the strain ε_2 (the second principal strain) is introduced into the micromodel as a constant. The principal strain ε_1 and the work pressure p are also used in the micromodel of the RVE.

3. Results

The results obtained for macromodels POLVAD and POVAD_EXT in our own FEM code and ABAQUS code are shown in figures 6 and 7 as the distributions of effective strain and effective stress under working loadings. The biggest values of effective strain and effective stress in the wall of blood chamber under working loadings are observed on the inner surface of a bottom part of blood chamber between two connectors. The computed effective strains are in linear elastic zones of the values for polyurethane in both versions of VAD. The results of simulations show the values of effective stress equal tens of kPa on the wall of blood chamber, which in comparison with the working loadings applied (subchapter 2.3.1) and the material properties (subchapter 2.1) of chamber can be assumed as correct. The maximum values of all the parameters computed shown in table 1 and figures 6 and 7 are smaller for POVAD_EXT. A good agreement between the results computed in commercial and our own FEM codes is achieved.

The results given below were transferred from macroscale to microscale as boundary conditions. We obtained these results based on the probable failure zones located between two connectors in the material of the ventricular assist devices (figures 6 and 7):

i) POLVAD: principal strains ε_1 = 0.0002, ε_2 = 0.0001, pressure p = 16 kPa;

ii) POLVAD_EXT: principal strains ε_1 = 0.0001, ε_2 = –0.00005, pressure: p = 16 kPa.

The residual stress for both types of VAD was 500 MPa [3].

The results obtained from the micromodel of TiN/PU specimen for POLVAD and POLVAD_EXT (table 2 and figures 8–9) show that the highest tensile stresses are generated in POLVAD. The rest of the parameters computed for micromodel are comparable in value for both types of VAD. The effective strains calculated are in linear elastic zones of the values for the materials used in both types of VAD (subchapters

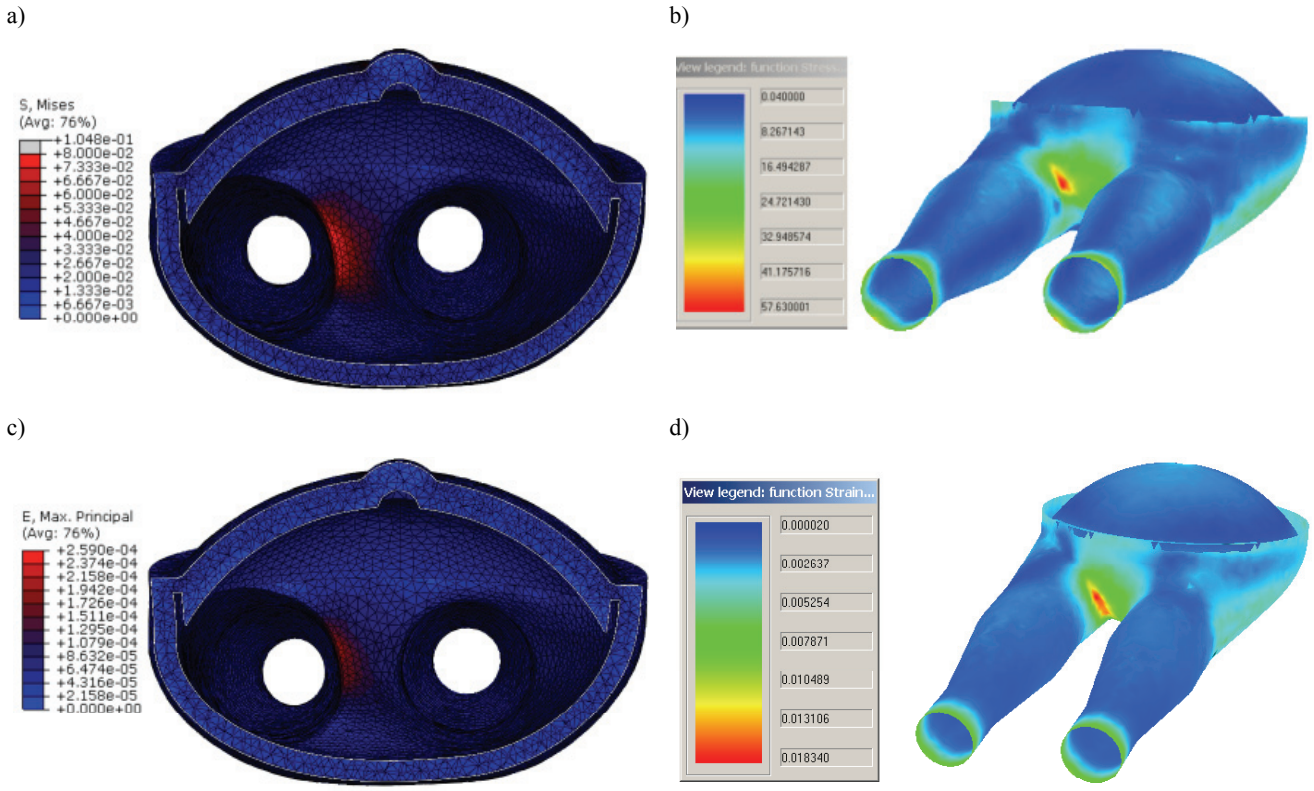

Fig. 6. POLVAD: distributions of effective stress obtained in: ABAQUS in MPa (a), our own code in kPa (b), and effective strain (in our own FEM code ×100) in: ABAQUS (c), our own code (d)

Table 1. Maximum values of selected parameters computed for macromodels of POLVAD and POLVAD_EXT in our own FEM code and ABAQUS

Parameter	POLVAD		POLVAD_EXT	
	Our own FEM code	ABAQUS	Our own FEM code	ABAQUS
Effective strain	0.00016	0.00019	0.00011	0.000105
Effective stress, kPa	58	68	33	35
Pressure, kPa	31	35	14	16

Table 2. Maximum values of selected parameters computed for micromodels of POLVAD and POLVAD_EXT in our own FEM code

Parameter	POLVAD		POLVAD_EXT	
Effective strain	0.001591		0.001416	
Stress	tensile (+)	compressive (–)	tensile (+)	compressive (–)
Average stress, MPa	0.21	366	0.12	385
Stress in *X* direction, MPa	155	395	86	406

2.1–2.2 and figure 1). The parameters of bilinear elastic-plastic material model selected for TiN are identified in inverse analysis by using the model of nanoindentation test (figure 1 and subchapter 2.2). In the simulations carried out for the micromodel of TiN/PU specimen, the greatest values of the parameters computed and their gradients occur in the nanocoating and between nanocoating and substrate. Thus, an experimental investigation of the quality of materials connection during long-time work of blood chamber proves clearly justified. Due to a lack of an adequate number of experimental results necessary to estimate the residual stress in nanocoating and the distribution of strain in a material of blood chamber, the macro- and micro-results obtained should be considered more qualitatively rather than quantitatively at this stage of project.

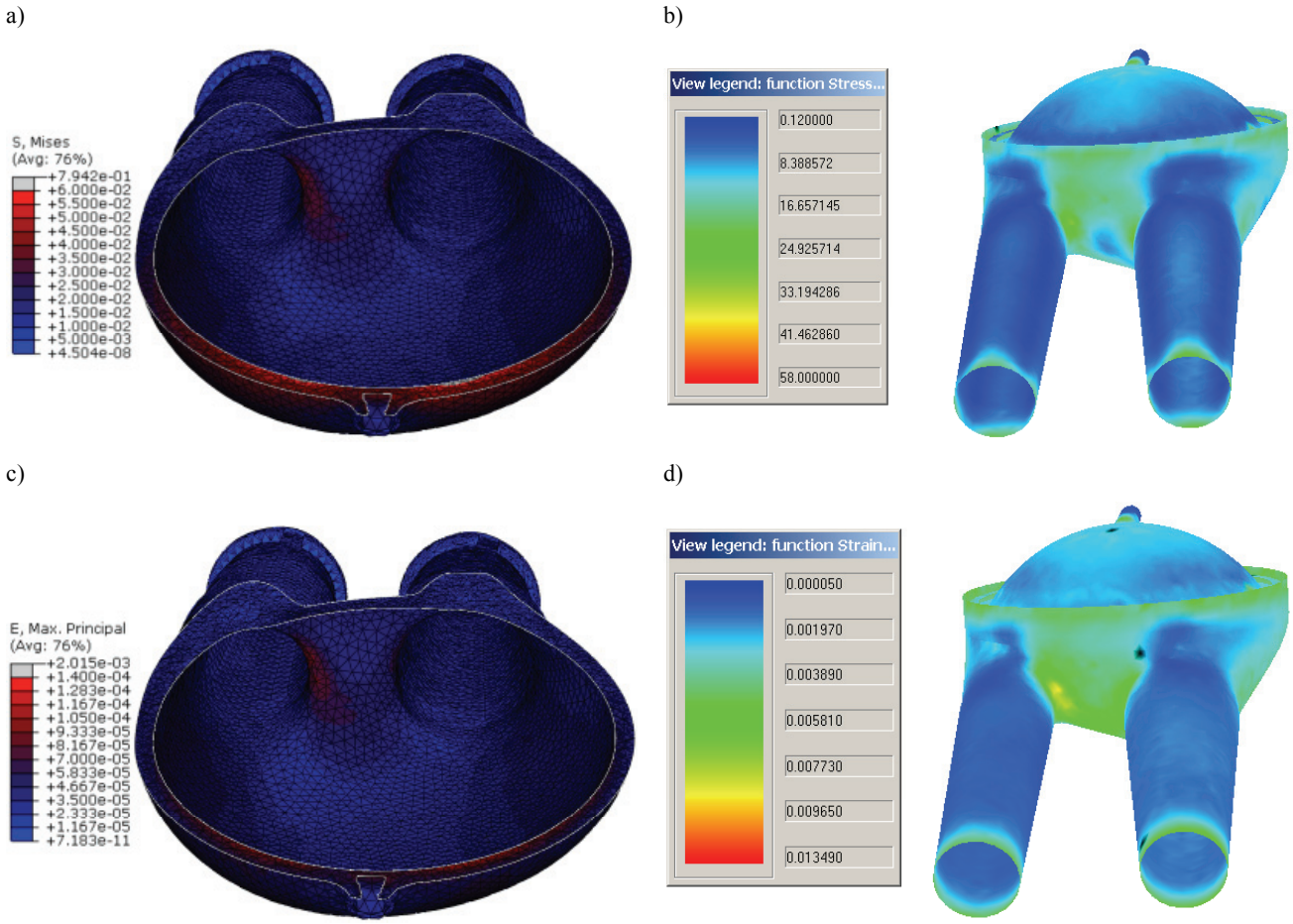

Fig. 7. POLVAD_EXT: distributions of effective stress obtained in: ABAQUS in MPa (a), our own code in kPa (b) and effective strain (in our own FEM code ×100) in: ABAQUS (c), our own code (d)

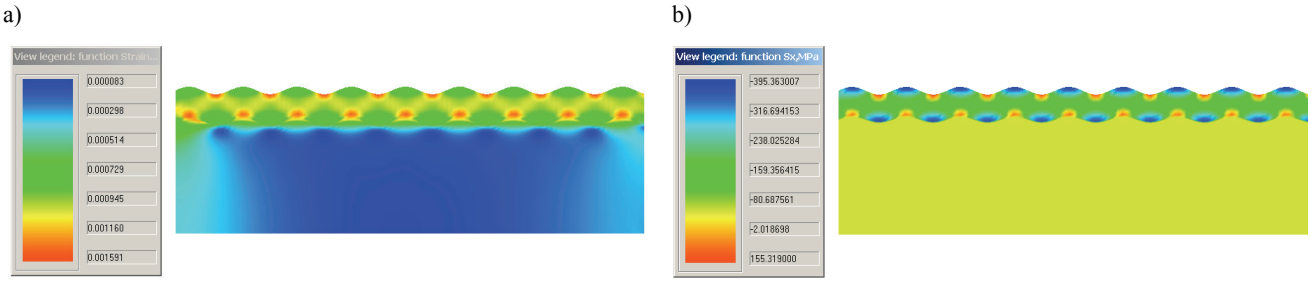

Fig. 8. Distributions of: effective strain (a) and stress in *X* (longitudinal) direction in MPa (b) in micromodel of TiN/PU specimen of POLVAD

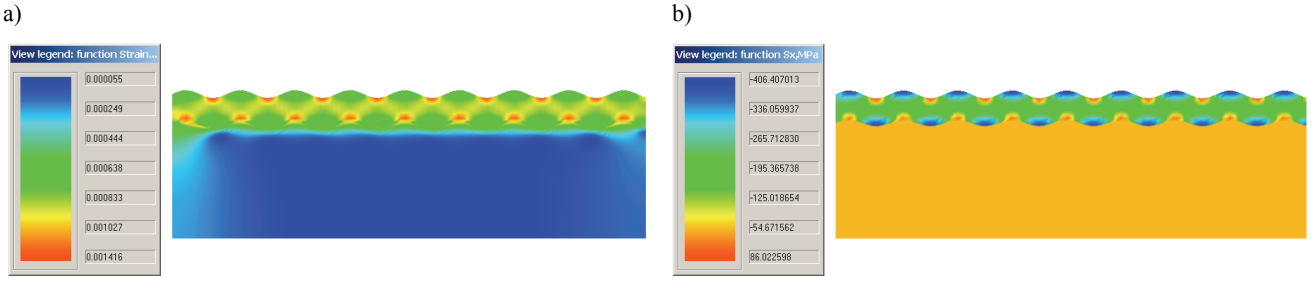

Fig. 9. Distributions of: effective strain (a) and stress in *X* (longitudinal) direction in MPa (b) in micromodel of TiN/PU specimen of POLVAD_EXT

4. Discussion of results

The macromodel of VAD should make it possible to predict the stress and strain states in the applied material after active loading. The model allows simulating the wall of VAD by using the nonlinear elastic properties, which are reached in standard experimental studies (tension test). The TiN nanocoating (elastic-plastic properties identified in the model of nanoindentation test) can also be simulated. Besides, the program allows the simulation of a partial or total unloading of the material of VAD, which plays a crucial role while using cyclic loading.

The goal of performing simulations for VAD macromodel was to compare two models of VADs: POLVAD and POLVAD_EXT and to verify the results in macroscale by using ABAQUS, a commercial FEM program. The results computed show a good agreement between our own and commercial codes (table 1 and figures 6–7). The results reached in our own code for macromodel of POLVAD were presented partially in [3], and for POLVAD_EXT in figure 7. The comparison of simulation data indicates that our own code can be used for VAD simulation, which in the nearest future will be also validated by using experimental data reached in extensometer studies.

The highest values of stress and strain are observed in the regions between two connectors of VAD (figures 6 and 7). The effective strains computed are in linear elastic zones of the values for polyurethane in both types of VAD. The comparison between the older type of VAD – POLVAD and the latest one – POLVAD_EXT indicates that the latter is designed to reach smaller values of stresses and strains (table 1). The comparison of the results for solid macromodel of VADs with those from literature is not possible. For example, the results for VAD shown in [18] are computed only for blood flow in chamber, just the same as the rest of data presented in literature for VADs. There is no data for the solid multiscale model of VAD composed of substrate and nanocoating. The developed model of VAD is unique because of the deposited nanocoating, which is not done by other researchers. Consequently, it is not interesting what happens in the solid macromodel of VAD without coating, because only nanocoating/substrate tends to start cracking, delaminating, etc.

The micromodel of the wall of VAD developed by our own FEM computer program is helpful in reaching the following goals:

i) Identification of the parameters in material model of TiN nanocoating.

ii) Identification of the residual stress state in TiN nanocoating.

iii) Simulation of stress and strain states in the specified regions (failure-source regions) of the wall of VAD.

The results reached for the first case were presented in subchapter 2.2 as the values of parameters in selected material model of TiN nanocoating. Based on these results the Young's modulus for TiN was calculated and proved to be comparable to the values obtained in the review of literature shown in [13]. The output of the model developed for nanoindentation test corresponds to the experimental data (figure 1). This is caused mainly by a correct reproduction of unloading phase after active loading phase in the model of nanoindentation test and using elastic-plastic and nonlinear elastic properties of specimen materials [13]. The understanding of the plastic properties in microscale model will be very important to predict cracking phenomena, especially between TiN nanocoating and PU substrate in the long-term cyclic loading applied in the VADs.

The residual stress state in the micromodel of VAD wall composed of TiN/PU is defined on the basis of experimental studies (FEM) and inverse analysis [13] (figure 2a). In the micromodel applied in [3], the value of residual stress state reaches 0.5 GPa, which in comparison with stresses generated in the macromodel of VAD after active loading is a very high value (figures 6–7 and table 1). Taking into account the high values of residual stresses plays a crucial role in the modelling because of cyclic loading, which can cause propagation of cracking in the boundaries between substrate and nanocoating.

The maximum gradients of stresses are observed in nanocoating and on the boundaries of substrate/nanocoating in micromodel (figures 8–9 and table 2), which can lead to cracking. The smaller values of tensile stresses are reached in micromodel of POLVAD_EXT. The highest values of effective strain in micromodel are comparable for both types of VAD and occur in linear elastic zones of the values for both materials of VADs. The strain state computed in the VAD after loading is subsequently transferred into micromodel (figure 2b) which is an important step in the active loading modelling in the micromodel of VAD wall.

Recapitulating, the micromodel of the wall of VAD takes into account residual stress state resulting from the deposition of coating (subchapter 2.2), complete material model of the deposited coating and stresses resulting from working loadings of VAD. The micromodel is applied in the macromodel of VAD

where the maximum values of strain and stress are observed – between two connectors (the most probable failure-source regions). The validation of the micromodel developed by using experimental data is not possible in this stage of the research, but is considered to be done in the nearest future. There is also little data in the literature which can be used to quantitative or qualitative comparison of microscale results. It should be emphasized that all the experimental studies carried out in very small scale are highly erroneous and such errors cannot be eliminated by numerous tests only. For example, the methodology of estimating the residual stress state is controversial, thus all the results presented in nanoscale should be considered probable, but not perfectly correct. Therefore, we are convinced of the necessity for developing numerical models, because they allow analyzing different values of parameters and their influence on model [13] (sensitivity analysis and optimization procedures), which in the absence of a full confidence in the experimental studies seems to be appropriate.

The developed multiscale FEM model of VAD in our own computer program is a stage of FSI (fluid structure interaction) solution [4], [5]. The pressure of blood flowing through the chamber interacts with the wall, and then this pressure is exerted on the inner surface of the macromodel. In the reverse direction, the reaction of chamber wall to the blood flow also takes place, but it is incomparably slower. The prepared multiscale FEM model of VAD is also considered to be used in the optimization of the parameters of material models for other nanocoatings and substrates, different thicknesses of deposited nanocoatings, the specified parameters of the geometry of VAD, in terms of designing the connectors, the analysis of blood flow without stagnation zones and turbulences.

5. Conclusions

i) The biggest contribution to Polish mechanical circulatory support represented by several constructions of VAD is now made by Polish Artificial Heart Programme.

ii) The construction nanomaterials for VAD are biocompatible nanocoatings such as Ti, TiN and TiCN.

iii) The experimental nanotechniques of measurement and identification of key mechanical properties of nanomaterials are applied in VADs' construction.

iv) The selected multiscale methods (finite element method, inverse analysis and representative volume element) are used in the proposed multiscale model of VAD.

v) The finite element solution based on our own code reproduces the strain and stress states in the VAD blood chamber. The distributions of the parameters selected help to define precisely the regions of chamber, which can be defined as the failure-source areas.

vi) The micromodel based on our own FEM code is composed of substrate material (PU) and TiN nanocoating. The distributions of stress and strain states help to determine the critical values of these parameters, which can be achieved in the nanomaterials tested.

vii) The analysis of strain–stress state for macro- and micromodels of both VADs (POLVAD and POLVAD_EXT) reveals smaller values of critical parameters computed for POLVAD_EXT than for POLVAD. Therefore, the construction of POLVAD_EXT seems to be better than that of POLVAD. However, all values of strain are reached only in linear elastic zones for both types of VADs in macro- and microscales.

Acknowledgements

Financial assistance of the MNiSzW, project No. 08/WK/P02/0001/SPB-PSS/2008, is acknowledged. The authors of the present paper participate in the "Polish Artificial Heart Programme" and perform the task: "Numerical model of totally implantable pulsatile ventricular assist device". Calculations in ABAQUS FEM program were made in ACK CYFRONET AGH, calculation grant No. MNiSW/IBM_BC_HS21/AGH/020/2008.

Literature

[1] JONES M.I., MCCOLL I.R., GRANT D.M., PARKER K.G., PARKER T.L., *Protein adsorption and platelet attachment and activation on TiN, TiC, and DLC coatings on titanium for cardiovascular applications*, J. Biomed. Mater Res., 2000, 52, 413–421.

[2] EBNER R., LACKNER J.M., WALDHAUSER W., MAJOR R., CZARNOWSKA E., KUSTOSZ R., LACKI P., MAJOR B., *Biocompatibile TiN-based novel nanocrystalline films*, Bull. Pol. Ac. Tech., 2006, 54, 167–173.

[3] MILENIN A., KOPERNIK M., *FEM code for the multi-scale simulation of the stress–strain state of the blood chamber composed of polyurethane and TiN nanocoating*, Comput. Meth. in Mater. Sci., 2011, 11, 215–222.

[4] HANSBO P., *Space-time oriented streamline diffusion methods for nonlinear conservation laws in one dimension*, Commun. Numer. Methods Eng., 1994, 10, 203–215.

[5] DONEA J., HUERTA A., PONTHOT J.P., RODRÍGUEZ-FERRAN A., *Arbitrary Lagragian–Eulerian methods, Encyclopedia of Computational Mechanics*, Stein E., de Borst R. and Hughes T. (editors), John Wiley&Sons, 2004, 1, 413–437.

[6] MILENIN A., KOPERNIK M., *The muliscale FEM model of artificial heart chamber composed of nanocoatings*, Acta Bioeng. Biomech., 2009, 11, 13–20.

[7] PAULEAU Y., *Generation and evolution of residual stresses in physical vapour-deposited thin films*, Vacuum, 2001, 61, 175–181.

[8] KOPERNIK M., KOT R., *The multiscale modeling of thin films growth*, Hutnik, 2010, 8, 403–406.

[9] SARNA J., KUSTOSZ R., MAJOR R., LACKNER J.M., MAJOR B., *Polish Artificial Heart – new coatings, technology, diagnostics*, Bull. Pol. Ac. Tech., 2010, 58, 329–335.

[10] PARK J., KIM D.J., KIM Y.K., LEE K.H., LEE K.H., LEE H., AHN S., *Improvement of the biocompatibility and mechanical properties of surgical tools with TiN coating by PACVD*, Thin Solid Films, 2003, 435, 102–107.

[11] CHIEN C.C., LIU K.T., DUH J.G., CHANG K.W., CHUNG K.H., *Effect of nitride film coatings on cell compatibility*, Dent. Mater., 2008, 24, 986–993.

[12] SERRO A.P., COMPLETO C., COLAÇO R., SANTOS F., LOBATO da SILVA C., CABRAL J.M.S., ARAÚJO H., PIRES E., SARAMAGO B., *A comparative study of titanium nitrides, TiN, TiNbN and TiCN, as coatings for biomedical applications*, Surf. Coat. Tech., 2009, 203, 3701–3707.

[13] KOPERNIK M., MILENIN A., MAJOR R., LACKNER J.M., *Identification of material model of TiN using numerical simulation of nanoindentation test*, Mater. Sci. Tech., 2011, 27, 604–616.

[14] FISCHER-CRIPPS A.C., *Nanoindentation*, Springer-Verlag, Lindfield, Australia, 2002.

[15] De BORST R., *Challenges in computational materials science, multiple scales, multi-physics and evolving discontinuities*, Comp. Mat. Sci., 2008, 43, 1–15.

[16] MILENIN A., MUSKALSKI Z., *The FEM simulation of cementite lamellas deformation in pearlitic colony during drawing of high carbon steels*, The Proc. Conf. Numiform., Cesar de Sa J.M.A. and Santos A.D. (editors), Porto, 2007, 1375–1380.

[17] ZIENKIEWICZ O.C., TAYLOR R.L., *The finite element method*, Butterworth-Heinemann, London, 2000.

[18] MOOSAVI M.-H., FATOURAEE N., KATOOZIAN H., *Finite element analysis of blood flow characteristics in a ventricular assist device (VAD)*, Simul. Model. Pract. Th., 2009, 17, 654–663.

[19] SACKS M.S., MERRYMAN W.D., SCHMIDT D.E., *On the biomechanics of heart valve function*, J. Biomech., 2009, 42, 1804–1824.

[20] LITWIŃSKI P., WOŹNIEWICZ B., RELIGA G., PASTUSZEK M., PARULSKI A., JASIŃSKA M., KOCAŃDA S., KUSTOSZ R., SIONDALSKI P., RELIGA Z., *Zastosowanie mechanicznego wspomagania krążenia sztucznymi komorami typu POLVAD w leczeniu wstrząsu kardiogennego na tle zapalenia mięśnia sercowego*, Kardiochir. Torakochir. Pol., 2005, 2, 33–40.

[21] MILENIN A., *Podstawy metody elementów skończonych*, Akademia Górniczo-Hutnicza, Kraków, 2010.

[22] IRONS B.M., *A frontal solution program for finite element analysis*, Int. J. Numer. Meth. Eng., 1975, 3, 293–294.

[23] TORQUATO S., *Random heterogeneous materials: microstructure and macroscopic properties*, Springer-Verlag, New York, 2002.

[24] ZOHDI T.I., WRIGGERS P., *Introduction to Computational Micromechanics*, Springer Series, [in:] *Lecture Notes*, Appl. Comput. Mech., 2005, 20.

[25] HILL R., *On constitutive macro-variables for heterogeneous solids at finite strain*, Proc. R. Soc. Lond., 1972, 326, 131–147.

[26] THIBAUX P., CHASTEL Y., CHAZE A.-M., *Finite element simulation of a two-phase viscoplastic material: calculation of the mechanical behaviour*, Comput. Mater. Sci., 2000, 18, 118–125.